



LETTER

Landscape process domains drive patterns of CO₂ evasion from river networks^{ab}

Gerard Rocher-Ros ,* Ryan A. Sponseller ,¹ William Lidberg ,² Carl-Magnus Mörth ,³ Reiner Giesler

¹Climate Impacts Research Centre, Department of Ecology and Environmental Science, Umeå University, Abisko, Sweden;

²Department of Forest Ecology and Management, Swedish University of Agricultural Science, Umeå, Sweden; ³Department of Geological Sciences, Stockholm University, Stockholm, Sweden

Scientific Significance Statement

CO₂ evasion from river networks is an important flux in the global carbon cycle, yet global estimates are largely unconstrained. This uncertainty reflects the challenge of understanding landscape patterns of the two underlying drivers of CO₂ evasion from streams: the concentration of CO₂ in water, and the turbulent flows that promote gas transfer to the atmosphere. Here, we show that, while transfer rates regulate where gas losses can occur in streams, it is the CO₂ concentration in the water that ultimately controls variation in the magnitude of evasion. Landscape topography emerges as an overarching driver that dictates the spatial arrangement of these two controls. Recognizing these fine scale spatial patterns is critical for future global upscaling of CO₂ evasion from river networks.

Abstract

Streams are important emitters of CO₂ but extreme spatial variability in their physical properties can make upscaling very uncertain. Here, we determined critical drivers of stream CO₂ evasion at scales from 30 to 400 m across a 52.5 km² catchment in northern Sweden. We found that turbulent reaches never have elevated CO₂ concentrations, while less turbulent locations can potentially support a broad range of CO₂ concentrations, consistent with global observations. The predictability of stream pCO₂ is greatly improved when we include a proxy for soil-stream connectivity. Catchment topography shapes network patterns of evasion by creating hydrologically linked “domains” characterized by high water-atmosphere exchange and/or strong soil-stream connection. This template generates spatial variability in the drivers of CO₂ evasion that can strongly bias regional and global estimates. To overcome this complexity, we provide the foundations of a mechanistic framework of CO₂ evasion by considering how landscape process domains regulate transfer and supply.

*Correspondence: g.rocher.ros@gmail.com

Associate editor: James Heffernan

Author Contribution Statement: G.R.R., R.G., and R.A.S. designed the study and wrote the paper. G.R.R. carried out the field work, processed and analyzed the data and W.L. provided the wetness data. C.M.M. and W.L. provided scientific insight to the analysis and interpretation of the data. R.G. contributed funding. All authors commented on the earlier versions of this manuscript.

Data Availability Statement: Data and metadata used in this study are available in the Swedish National Data Service (<https://doi.org/10.5878/pxa2-vy55> and <https://doi.org/10.5878/77ps-4f21>). The code to reproduce the figures and the results is deposited in GitHub (https://github.com/rocher-ros/co2_domains_publication).

Additional Supporting Information may be found in the online version of this article.

This is an open access article under the terms of the Creative Commons Attribution License, which permits use, distribution and reproduction in any medium, provided the original work is properly cited.

CO₂ evasion is the largest pathway for carbon (C) loss from inland waters (Cole et al. 2007), with a total flux that matches net oceanic uptake. Particularly important are streams and rivers, which account for more than 85% of CO₂ evasion while only covering 17% of the inland water surface (Raymond et al. 2013). Yet, current global estimates of CO₂ evasion from running waters are remarkably unconstrained (Drake et al. 2017), with a threefold difference among studies, ranging from 0.7 (Lauerwald et al. 2015) to 1.8 Pg C yr⁻¹ (Raymond et al. 2013), despite using the same data source (Hartmann et al. 2014). We suggest that this uncertainty is related to how we conceptually treat the two fundamental variables underlying CO₂ evasion: the partial pressure of water CO₂ ($p\text{CO}_2$) and the gas transfer velocity, k_{600} , a measure that reflects water's turbulence.

There have been major advances in upscaling k_{600} from fine scale measurements of stream morphology (Raymond et al. 2012), together with estimates of river area based on remote sensing (Allen and Pavelsky 2018). By comparison, we are still unable to predict $p\text{CO}_2$ and explain its variability over space and time. For instance, variability in $p\text{CO}_2$ is larger within small watersheds than across biomes (Wallin et al. 2018), and river size is a poor predictor of $p\text{CO}_2$ in the current global data set (Marx et al. 2017). To overcome this problem, current approaches for upscaling (Butman and Raymond 2011; Raymond et al. 2013; Borges et al. 2015; Wallin et al. 2018) typically involve estimating $p\text{CO}_2$ from aggregated water chemistry data over large regions and matching this with more finely resolved estimates of k_{600} . However, summarizing $p\text{CO}_2$ and k_{600} at different scales may result in erroneous estimates of CO₂ evasion because these underlying parameters may not be independent. Therefore, to upscale CO₂ evasion from streams, we need to develop robust tools to predict $p\text{CO}_2$ and k_{600} at similar spatial scales.

Concentrations of CO₂ in streams reflect the dynamic balance of turbulent forces that promote evasion against multiple processes that resupply the system. On one hand, k_{600} can vary greatly within meters depending whether it is estimated within a pool, riffle, or waterfall (Keller and Melhorn 1978; Wallin et al. 2011) and this will constrain the rate at which CO₂ degassing can occur; henceforth defined as the transfer limitation. On the other hand, CO₂ is continuously added to streams through groundwater inputs (Öquist et al. 2009) and internal production (Hotchkiss et al. 2015), which can also vary markedly at small temporal (Peter et al. 2014; Crawford et al. 2016) and spatial scales (Natchimuthu et al. 2017; Wallin et al. 2018; Lupon et al. 2019). This rate of CO₂ supply could thus also limit evasion to atmosphere; henceforth defined as supply limitation. The extent to which transfer vs. supply limitation regulate patterns of CO₂ evasion remains ill-defined, despite being fundamental to a mechanistic understanding of evasion across stream networks. Here, we ask: to what extent does transfer vs. supply limitation shape network-scale patterns of CO₂ evasion, and how does resolving these underlying drivers influence our ability to upscale evasion rates to larger areas?

To answer this question, we estimated CO₂ evasion and its drivers at reach scales for a stream network in northern Sweden (the 52.5 km² Miellajokka catchment, Fig. 1a). The catchment

comprises a wide range of hydrological conditions and landscape properties and is thus suitable as a model system. We measured key hydrological parameters to estimate k_{600} , directly determined the $p\text{CO}_2$, and estimated CO₂ evasion across 168 sites in the stream network. Together with a quantification of wet areas in the catchment and other topographic information that might influence supply and/or transfer limitation, we assessed the drivers of the spatial variability in CO₂ evasion. We also utilize a global stream database (GLORICH; Hartmann et al. 2014) to test if our catchment-scale findings corroborate larger scale patterns observed for $p\text{CO}_2$, k_{600} , and evasion.

Material and methods

Site description

The Miellajokka catchment is in the arctic region in north-western Sweden (68°21'14"N, 18°56'16"E). The catchment covers 52.5 km², and elevation ranges between 384 and 1731 m above sea level (a.s.l.). The morphology of the catchment reflects several glaciations across millennia, which left behind U-shaped valleys and several deposits of coarse material and moraines. The broader landform of the catchment is characterized by steep peaks in the south, a large central plateau, and moderately sloped terrain that feeds an alluvial valley in the north (Fig. 1). The catchment is defined by four large streams which flow northward. The total length of the stream network is 44.6 km and includes first to fourth Strahler order streams (Supporting Information Table S1). Annual precipitation in Abisko (7 km from the study site, www.polar.se/abisko) for the period 1990–2013 was 337 mm, and the mean annual air temperature was 0.3°C. Land cover changes with elevation, from mostly bare rock above 1200 m a.s.l., to tundra vegetation between 700 and 1200 m, to sparse cover by mountain birch (*Betula pubescens* spp. *Czerepanovii*) and treeless tundra heath below the treeline at 700 m. Below 400 m, there are areas with more productive birch forest and denser canopy cover. Soil permafrost in this region is discontinuous at higher elevations and sporadic at low elevation areas. Bedrock is dominated by weakly metamorphic sedimentary rocks such as schist and dolomite in the central and western areas of the catchment, whereas more quarzitic and phyllitic hard schist and salic igneous rocks form bedrock along the eastern tributary.

Field sampling and analyses

We sampled 168 locations in this stream network between 11th and 20th of July 2016 (Fig. 1). The distance between sampling points increased with stream order as the travel time and velocity increases with channel size (Raymond et al. 2012); sampling locations were also constrained by having a suitable location to measure discharge (e.g., single channel, no pools). Thus, the distance between sites was between 30 and 100 m for first-order streams, between 100 and 200 m for second-order streams, and between 200 and 400 m for third- and fourth-order streams. Sampling was carried out between 08:30 h and 18:00 h every day. Weather conditions and flow levels across days were stable during this period,

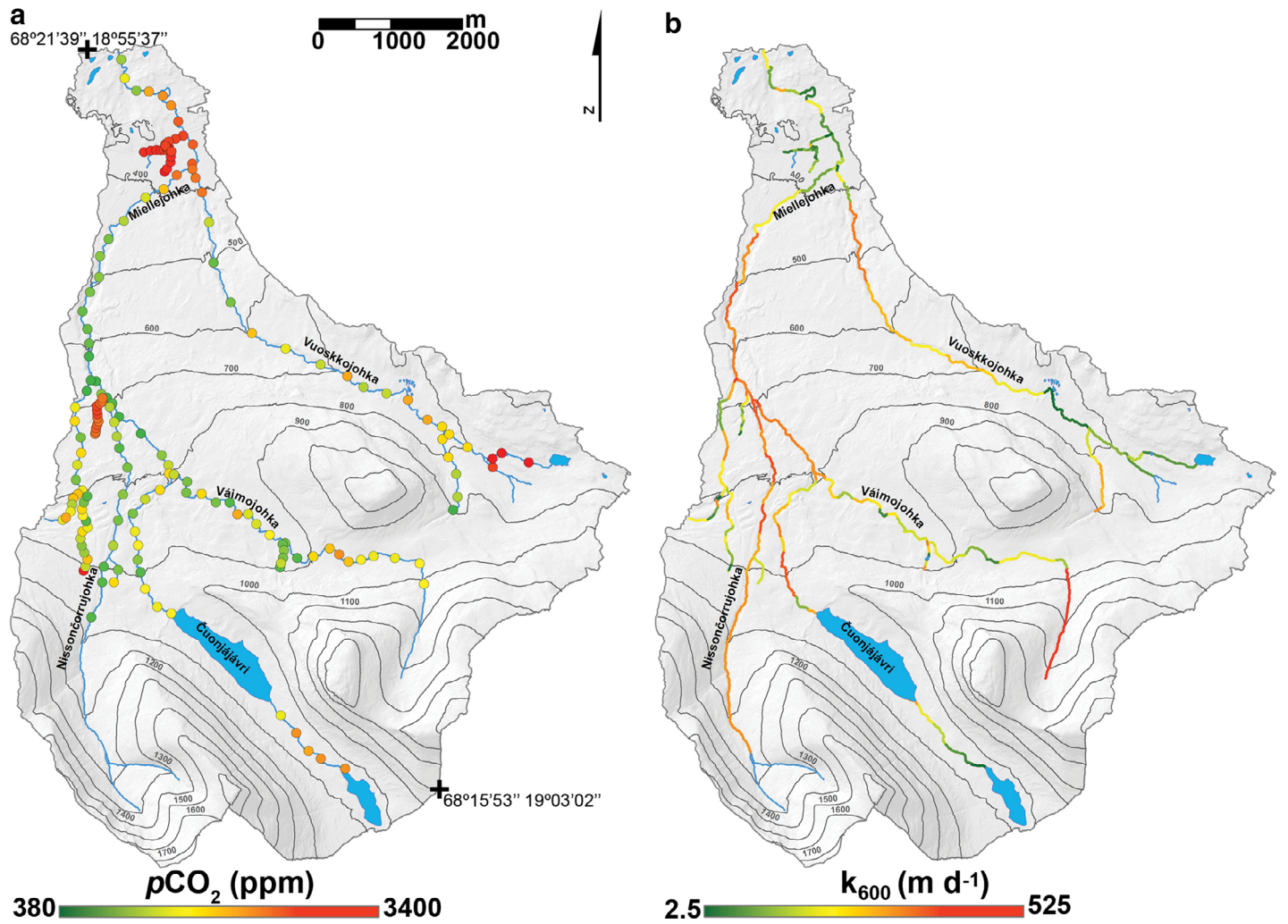


Fig. 1. Map of the Miellajokka catchment with the sampling sites and the measured $p\text{CO}_2$ (a) and modeled k_{600} (b) for each stream reach. The wetness map of the catchment is the Supporting Information Fig. S1.

with the coefficient of variation (as percentage) of discharge at the catchment outlet of 12.2%. In addition, daytime variation in $p\text{CO}_2$ during sampling hours was monitored at seven sites and was, in general, constant during this time of day (Supporting Information Fig. S3). There was some variability between days but this was small compared to the spatial variability (Supporting Information Fig. S3). At each sampling site, we measured water depth and velocity every 0.2 m along transects using an electromagnetic flow meter (model 801 EC Meter; Valeport, Devon, U.K.). We also measured $p\text{CO}_2$ in situ using a handheld device (Vaisala DM70, Helsinki, Finland) adapted for wet environments as in Johnson et al. (2010) and water temperature with a handheld thermometer. Stream discharge was calculated as the product of the cross-section area and the velocity of the stream. CO₂ concentrations measured with the Vaisala instrument (accuracy of ± 10 ppm) need to be corrected for air pressure and temperature (Johnson et al. 2010). Specifically, the sensor output has to be corrected by 0.15% per hPa departure from 1013 hPa, and by

-0.3% per °C difference from 25°C, as stated in Johnson et al. (2010). The flux of CO₂ to the atmosphere was calculated as:

$$F_{\text{CO}_2} = k_{\text{CO}_2} \times \Delta\text{CO}_2 \quad (1)$$

where k_{CO_2} is the gas transfer velocity for CO₂, and ΔCO_2 is the difference in CO₂ concentration between the water and the air. We used an air CO₂ concentration of 380 ppm based on measured concentrations with the handheld device at the six monitoring sites. The air concentration was the same (380 ppm) at each site. The k_{CO_2} was calculated as:

$$k_{\text{CO}_2} = \left(\frac{\text{Sc}_{\text{CO}_2}}{600} \right)^{-1/2} / k_{600} \quad (2)$$

where Sc_{CO_2} is the Schmidt number for CO₂ at the water temperature calculated following the coefficients summarized in Raymond et al. (2012) and k_{600} is the gas transfer velocity standardized for a Schmidt number of 600. Due to the impossibility of

directly measuring k_{600} at a large spatial extent, we used measured hydraulic parameters to estimate the gas transfer velocity for each reach, based on the relationship following Raymond et al. (2012):

$$k_{600} = 4725 \pm 445 \times (V \times S)^{0.86 \pm 0.016} \times Q^{-0.14 \pm 0.012} \times D^{0.66 \pm 0.029} \quad (3)$$

where V is the water velocity (m s^{-1}), S is the slope (unitless), Q is discharge ($\text{m}^3 \text{s}^{-1}$), and D is depth (m). To obtain k_{600} for the global database GLORICH, we derived the slope for each site and calculated k_{600} using velocity and slope as predictors. The $p\text{CO}_2$ used from the GLORICH database (Hartmann et al. 2014) was processed as follows: first we calculated the median value if several per site were available, then we excluded sites with unclear geographical coordinates and/or with $p\text{CO}_2 > 40,000$ ppm, which gave us a total of 4790 sites. A full description of the data used as well as the modeling of k_{600} can be found in the Supporting Information Text S1.

We used the digital elevation model at a resolution of 2 m to derive a depth to water index for the Miellajokka Catchment (DTW; details of the computations can be found in Supporting Information Text S2). Wet areas were defined as locations where the distance to the water table was less than 1 m, suggesting stronger connectivity to the stream network (Lidberg et al. 2017). For each site, wet area was computed as the percent cover of the incremental catchment area from the previous upstream site with a DTW < 1 m. A source of error when estimating the effect of wet areas for a given reach is that the travel distance of a gas may be longer than the distance to the upstream sampling site, and therefore integrate the properties from that upstream site. We calculated the mean travel distance of a gas entering the stream as $0.7 \times V/K_{600}$ (V in m d^{-1} , and K_{600} is k_{600}/D in d^{-1}) following Demars et al. (2015), and found that the median integration distances for first-, second-, third-, and fourth-order streams were 44 m, 78 m, 86 m, and 678 m, respectively. These values are similar or smaller than the distance between the sampling sites.

Statistical analysis

We completed all statistical analyses in R (version 3.5.1), using the *lm()* function for linear and multiple regressions, and *ggplot2* (version 3.0.0) for visualization. To assess the relative importance of k_{600} and $p\text{CO}_2$ on CO₂ evasion, we used a multiple linear regression with the variables standardized and log-transformed. Accordingly, Eq. 1 defined in log-space becomes: $\log(F_{\text{CO}_2}) = \log(k_{\text{CO}_2}) + \log(\Delta\text{CO}_2)$, and in a multiple linear regression (i.e., $\log(F_{\text{CO}_2}) = x_1 \times \log(k_{\text{CO}_2}) + x_2 \times \log(\Delta\text{CO}_2) + m$), the coefficients x_1 and x_2 are a measure of the relative importance of k_{CO_2} and ΔCO_2 to CO₂ evasion. To do this, we first standardized variables using the *scale()* function in R. Then, to calculate the partial R^2 for each independent variable, we used the function *modelEffectSizes()* of the package *lmSupport* (version 2.9.13), which provides the semi-partial correlation coefficients (r) and the partial coefficients of determination (R^2) for the two

independent variables. Finally, we used a bootstrapping exercise to explore the sampling intensity required to capture median CO₂ evasion from Miellajokka streams. Here, we randomly sampled the population of measurements assuming a variable sample size, from 1 to 168 (with sample replacement). This sampling was repeated 200 times for each sample size, and for each simulation, we calculated the median CO₂ evasion rate. The data sets used in the study are deposited in the Swedish National Data Service (<https://doi.org/10.5878/pxa2-vy55>) (Rocher-Ros 2019), and code to reproduce the results and figures is deposited in GitHub (https://github.com/rocher-ros/co2_domains_publication).

Results and discussion

Controls on CO₂ evasion from streams

In a worldwide data set of stream water chemistry (Hartmann et al. 2014), we find that CO₂ concentrations are always low (< 1000 ppm) at $k_{600} > 50 \text{ m d}^{-1}$, while there is large variation in stream $p\text{CO}_2$ below a k_{600} of 50 m d^{-1} (Fig. 2a). Thus, turbulent streams never have higher CO₂ concentrations, while less turbulent streams can potentially support a broad range of concentrations, from being in equilibrium with the atmosphere to concentrations above 20,000 ppm. Our empirical estimates from the Miellajokka catchment are remarkably consistent with this global observation. Across the 45 km long stream network (Fig. 1a,b), we consistently observed low CO₂ concentrations (< 500 ppm) at more turbulent stream reaches ($k_{600} > 100 \text{ m d}^{-1}$) while high $p\text{CO}_2$ values (> 1000 ppm) only were observed at a k_{600} below 100 m d^{-1} (Fig. 3a). The absence of high $p\text{CO}_2$ values at the more turbulent stream reaches suggests that the degassing rate is considerably larger than the supply of CO₂ that supports the evasion to the atmosphere. Hence, evasion from such stream reaches is likely to be supply rather than transfer limited as has been shown in other mountainous areas (Crawford et al. 2015).

While supply limitation prevents the build-up of higher stream CO₂ concentration in turbulent reaches, we also found that where $k_{600} < 100 \text{ m d}^{-1}$ stream $p\text{CO}_2$ exhibited large variation, with both high and low values (Fig. 3a). Thus, at similar transfer rates (e.g., similar k_{600}), the supply of CO₂ to streams varied markedly across this network. To explore the controls over this variability, we used the percentage of wet area draining into each site as a proxy for the strength of stream-groundwater connectivity (Kuglerová et al. 2014; Lidberg et al. 2017), assuming this also reflects the supply of C from riparian zones to streams (Hotchkiss et al. 2015; Tank et al. 2018; Lupon et al. 2019). We found that below a threshold of $k_{600} = 42 \text{ m d}^{-1}$ (Supporting Information Fig. S5), stream $p\text{CO}_2$ was significantly positively related to the % wet area in the adjacent riparian zone and this explained 63% of the variation in CO₂ concentrations (Fig. 3b). This relationship suggests a strong component of supply limitation on CO₂ evasion—even in streams with low turbulence, where CO₂ evasion should be primarily transfer limited. In contrast, only 23% of the variation in $p\text{CO}_2$ could be explained by the % wet area at k_{600} values above 42 m d^{-1} (Fig. 3b). This second

relationship most likely reflects the overarching influence of degassing, which at high exchange rates is able to mask the effects of variable supply to streams.

The balance between the supply and transfer shapes the overall relationship between k_{600} and $p\text{CO}_2$ (Fig. 3a). The nature of this relationship limits the predictability of $p\text{CO}_2$ when solely

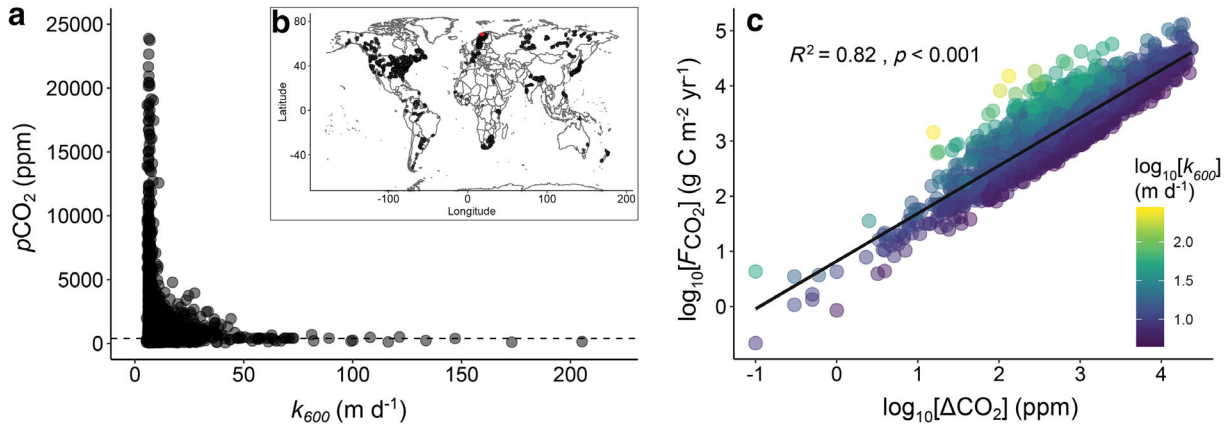


Fig. 2. Relationship between k_{600} and $p\text{CO}_2$ in the GLORICH data set (Hartmann et al. 2014) (a). The distribution of sites in the world (b), where the red dot shows the location of the Miellajokka catchment. (c) The relationship between excess $p\text{CO}_2$ relative to the atmosphere (ΔCO_2) and F_{CO_2} in the logarithmic scale, with symbol color representing k_{600} . The equation is $\log_{10}(F_{\text{CO}_2}) = 0.82 + 0.87 \times \log_{10}(\Delta\text{CO}_2)$.

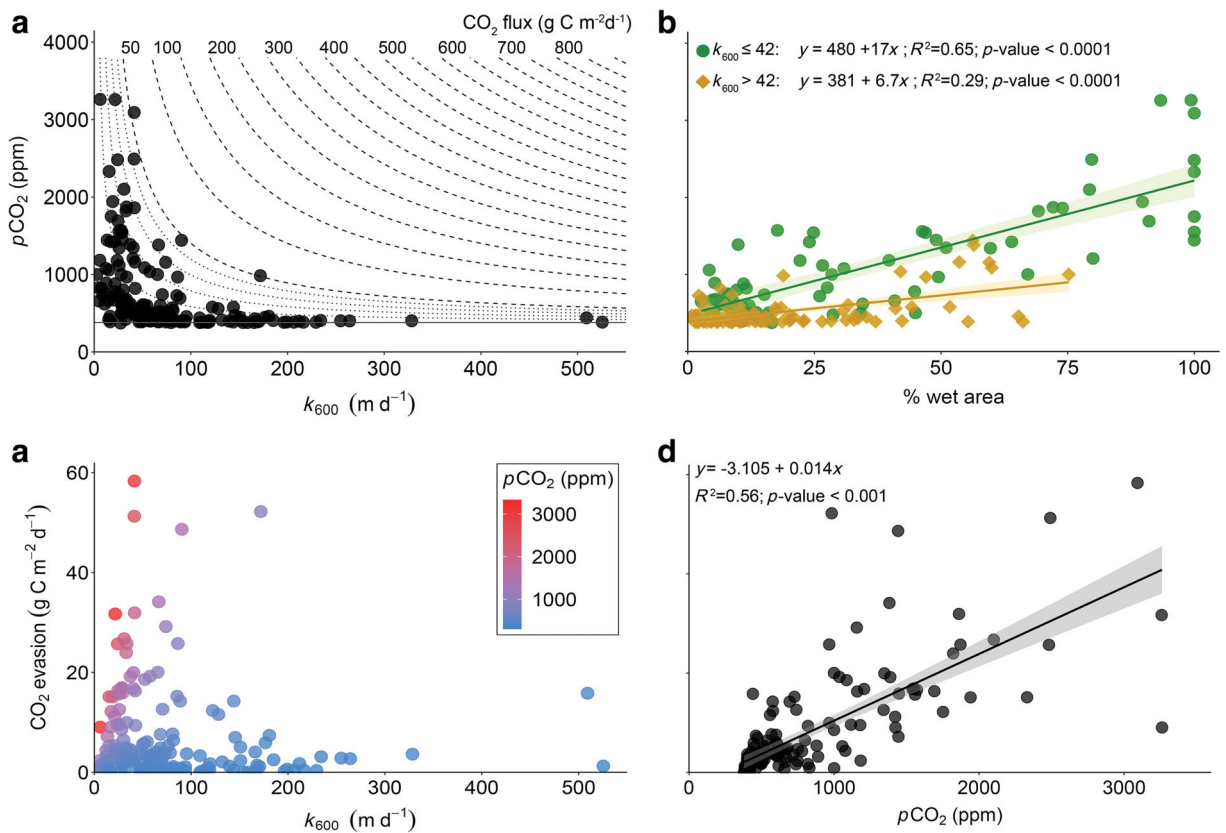


Fig. 3. Controls on stream $p\text{CO}_2$ and CO_2 evasion. (a) The relationship between k_{600} and $p\text{CO}_2$, following an inverse pattern. The dashed lines are isolines for CO_2 fluxes increasing by intervals of $50 \text{ g C m}^{-2} \text{ d}^{-1}$, the dotted lines intervals of $10 \text{ g C m}^{-2} \text{ d}^{-1}$ (shown below $50 \text{ g C m}^{-2} \text{ d}^{-1}$), and the solid line represents the atmospheric $p\text{CO}_2$. (b) The relationship between $p\text{CO}_2$ vs. the percentage of wet area draining into each site, for k_{600} smaller or larger than 42 m d^{-1} . (c) The relationship between CO_2 evasion rates and k_{600} , with symbols colored according to $p\text{CO}_2$. (d) The relationship between $p\text{CO}_2$ and CO_2 evasion.

based on k_{600} even if the two parameters are related (Fig. 3a). Indeed, including % wet area in a multiple linear regression greatly increased our ability to predict $p\text{CO}_2$ across all sites from 32% to 62% ($p\text{CO}_2(\text{ppm}) = 470 - 1.7 \times k_{600} + 17.9 \times \% \text{ wet area}$, $p < 0.001$). While we lack data to test this globally at such a fine scale, both catchment (Wallin et al. 2010) and continental scale (Borges et al. 2015) studies have similarly shown that wetland cover can explain patterns in riverine CO₂. Regardless, it is clear that the relationship we see between $p\text{CO}_2$ and k_{600} within a 52 km² catchment also holds at a global scale (Fig. 2a), suggesting a universal threshold of a k_{600} beyond which turbulent flows prevent the build-up of CO₂.

Understanding whether $p\text{CO}_2$ or k_{600} drives CO₂ evasion is necessary to upscale CO₂ emissions globally. Surprisingly, in the Miellajokka catchment, hotspots for CO₂ evasion are primarily found in stream reaches with lower k_{600} and not in the more turbulent reaches of the catchment (Fig. 3c). Importantly, CO₂ evasion rates are strongly related to $p\text{CO}_2$ in this catchment (Fig. 3d) and in the global data set (Fig. 2c). The importance of $p\text{CO}_2$ for evasion is also clear in the multiple linear regression. For the Miellajokka, the multiple linear regression was $\log(F_{\text{CO}_2}) = 0.62 \times \log(k_{\text{CO}_2}) + 1.27 \times \log(\Delta\text{CO}_2)$ ($R^2 = 0.98$, $p < 0.001$), with a partial R^2 of 0.89 for $\log(\Delta\text{CO}_2)$ and 0.04 for $\log(k_{\text{CO}_2})$. Thus, the higher coefficient (1.27 vs. 0.62) and the higher R^2 (0.89 vs. 0.04) of $\log(\Delta\text{CO}_2)$ compared to $\log(k_{\text{CO}_2})$ imply that $p\text{CO}_2$ is the critical driver of evasion and not k_{600} . Results from global data set were similar; here, the multiple linear regression was $\log(F_{\text{CO}_2}) = 0.42 \times \log(k_{\text{CO}_2}) + 1.01 \times \log(\Delta\text{CO}_2)$ ($R^2 = 0.97$, $p < 0.001$). The partial R^2 for $\log(\Delta\text{CO}_2)$ was 0.89 and for $\log(k_{\text{CO}_2})$ was 0.02. Together, these results highlight that constraining $p\text{CO}_2$ at fine spatial scales is essential to determine and upscale CO₂ evasion rates.

A turbulent stream reach is thus not a hotspot for CO₂ evasion by itself; our data suggest that such locations are instead found at reaches with moderate to low turbulence, but where there is sufficient supply of CO₂ to maintain higher stream concentrations and thus atmospheric losses. Importantly, while the supply of CO₂ to the water column emerges as the main driver of CO₂ evasion in these streams, the processes behind its origin are still uncertain (Hotchkiss et al. 2015). Some studies show that direct inputs of CO₂ produced in soils dominate this flux (Öquist et al. 2009), others highlight that near stream, riparian soils are the major source (Leith et al. 2015), while others still suggest that instream aquatic respiration can account for a large proportion of the CO₂ produced (Rasilo et al. 2016; Demars 2018). These are not mutually exclusive processes, and we are not able to resolve among them, as our measure of wetness index only captures variation in hydrological connectivity between land and water and changes in the lateral extent of riparian soils. These wet areas may foster higher rates of soil metabolism (Riveros-Iregui and McGlynn 2009) and directly supply streams with CO₂. At the same time, these zones may yield higher rates of lateral organic C supply, and thus support

higher rates of hyporheic (Pusch 1996) and/or benthic (Battin et al. 2008) respiration.

Process domains and CO₂ evasion in river networks

Overall, our results show that transfer limitation only regulates where CO₂ evades, while supply ultimately controls the magnitude of evasion. In the Miellajokka catchment, reaches with steeper channel slopes have greater turbulence and thus potentially elevated evasion rates, but only if there is sufficient CO₂ from internal production (e.g., aquatic respiration) or from lateral or upstream sources. By contrast, in many lower gradient reaches, riparian and groundwater features promote greater lateral C flux to streams and potentially elevated rates of aquatic metabolism and CO₂ production. Yet, such zones often lack the kinetic energy to support very high rates of CO₂ evasion. Thus, the true hotspots for evasion in the network likely emerge at the transitions between reaches characterized by high C supply and those by high turbulence—where high values of $p\text{CO}_2$ and k_{600} may coexist (Fig. 4). This perspective places new emphasis on longitudinal connectivity among transfer- and supply-limited reaches as a driver of C gas efflux. It has been suggested that the connectivity between lotic and lentic environments in the aquatic continuum creates a similar pattern (Hotchkiss et al. 2018), but here we suggest that these spatial interactions may operate at even finer scales within river networks.

While these spatial interactions likely generate unique patterns of CO₂ evasion for every catchment, the broader role of topography as the overarching driver of supply vs. transfer limitation in streams and rivers is general (Fig. 4). It is well recognized that shifts in topography along river systems generate discontinuities in geomorphic structure, or *process domains* that are characterized by unique hydrologic, edaphic, and ecological dynamics (Montgomery 1999). Moreover, recent studies have highlighted the fundamental roles that geomorphic structure plays as a regulator of C inputs (Duvert et al. 2018; Lupon et al. 2019), storage (Wohl et al. 2012), biological processing (Jankowski et al. 2014), and transport in river systems (Battin et al. 2008). Here, we provide evidence that simple topographic tools can help distinguish domains in the landscape where lateral C supply to streams is the dominant process driving gas evasion from others where turbulent flow and degassing are paramount. The transitions in these dominant processes underpin the fundamental dependence between $p\text{CO}_2$ and k_{600} that appears consistent at a global scale (Fig. 2a). Finally, we suggest that the relative position of these domains determines the location of hotspots for evasion in landscapes, which can also cause an extreme bias when upscaling gas evasion at regional or global scales. Our framework adds to the general understanding of C cycling in river networks, but also provides a set of guiding principles that will aid efforts to scale up CO₂ emissions from these systems.

Implications for upscaling

The effect of landscape domains can be very important when upscaling CO₂ evasion. Within the Miellajokka catchment CO₂

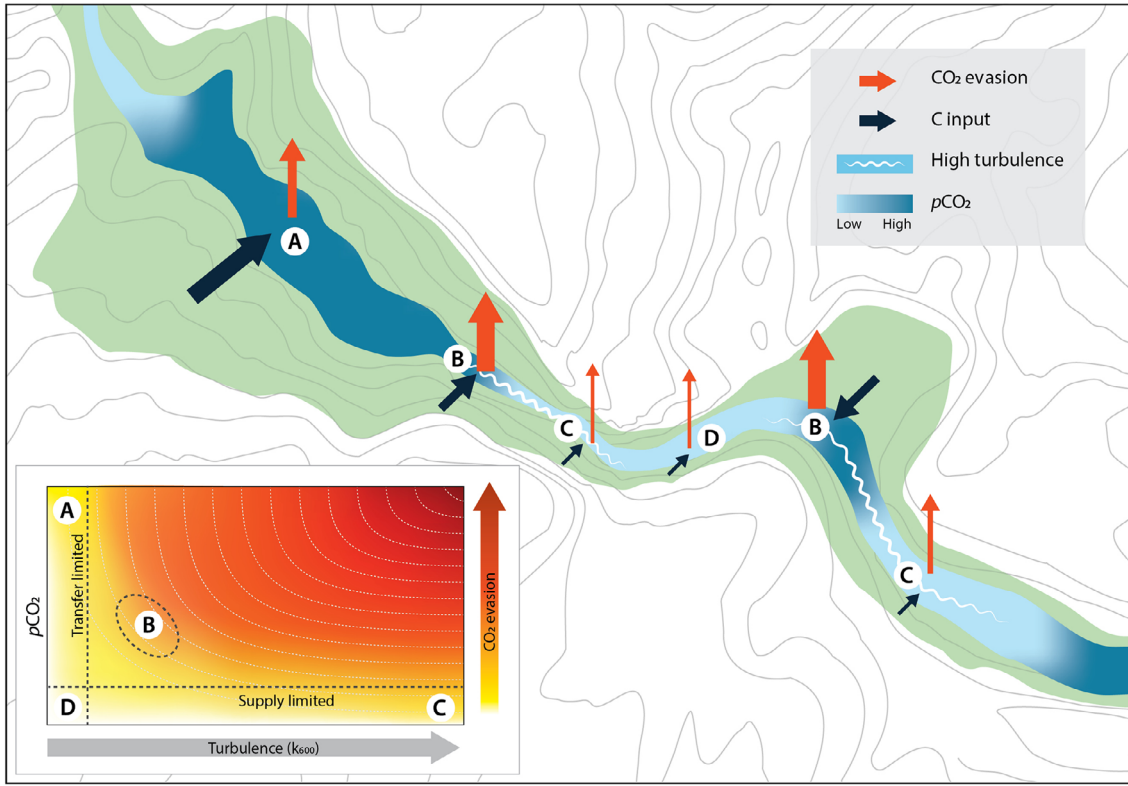


Fig. 4. Landscape process domains shaping CO₂ concentration and evasion rates in streams. pCO₂ can respond strongly to inputs of C from land or to outputs via evasion. The spatial arrangement of C inputs and turbulent areas determines the controls and the magnitude of CO₂ evasion. Thus, CO₂ evasion will be either transfer limited (A), supply limited (C) or both (D). Hotspots of CO₂ evasion can then occur when supply is high and there is enough turbulence to degas the water (B).

evasion ranged from 0 to 60 g C m⁻² d⁻¹, the latter among the highest evasion rates measured in northern streams (Natchimuthu et al. 2017) (Fig. 5b). Importantly, the distribution of these rates was highly skewed toward lower values (Fig. 5b), resulting in a large difference between the median and the mean estimate, 3.34 g C m⁻² d⁻¹ and 7.32 g C m⁻² d⁻¹, respectively. To what extent does this spatial heterogeneity in evasion rates also affect our ability to predict broader, catchment-scale CO₂ evasion estimates? The bootstrapping of the distribution of CO₂ evasion (Fig. 5a) shows that by collecting 10 samples from streams in this catchment would result in a large uncertainty, with a 5th–95th percentile of 1.43–8.02 g C m⁻² d⁻¹. Collecting 50 samples narrows this uncertainty to a 5th–95th percentile of 2.23–4.86 g C m⁻² d⁻¹, closer to the observed median of 3.34 g C m⁻² d⁻¹. As the catchment covers 52.5 km², these results then indicate that constraining catchment-scale estimates of CO₂ evasion would require roughly one sample for each square kilometer of catchment.

While the spatial variation in pCO₂ and k₆₀₀ is incorporated into the above estimates of CO₂ evasion, most current upscaling studies rely on estimates of pCO₂, k₆₀₀, and stream area that are determined at different scales. If we apply a similar approach to the Miellajokka catchment and use the median k₆₀₀ determined from stream morphology across the catchment and pCO₂

measured at the main stem outlet (which is also a national monitoring station), the estimated CO₂ evasion is 54.7 g C m⁻² d⁻¹ (red triangle in Fig. 5a), more than 15-fold higher than the median flux. These differences in the parameters to estimate CO₂ evasion will thus result in a grossly overestimated catchment CO₂ evasion. In our case, we overestimate evasion, due to the high median catchment k₆₀₀ (54.5 m d⁻¹) and high pCO₂ in the monitoring station as it is located in a flat and moist area (1180 ppm, site M1 in Supporting Information Fig. S1), but the direction of this bias could go either way. This exercise highlights that the scale at which parameters are estimated can strongly affect the evasion estimate. For example, Raymond et al. (2012) calculated riverine CO₂ evasion globally using pCO₂ from the GLORICH database but used topographic data at finer spatial scales to determine the k₆₀₀, obtaining a CO₂ evasion rate of 3358 g C m² yr⁻¹ (total riverine CO₂ evasion divided by the reported riverine area). In this study, we calculated the k₆₀₀ and the CO₂ evasion at the sites of the GLORICH database where pCO₂ was measured, obtaining a median evasion rate of 1670 g C m² yr⁻¹, about half of the estimate by Raymond et al. (2012). Our measure is much closer to the estimate of riverine CO₂ evasion of 1574 g C m² yr⁻¹ from Lauerwald et al. (2015), which upscaled pCO₂ and k₆₀₀ at the same spatial scales although

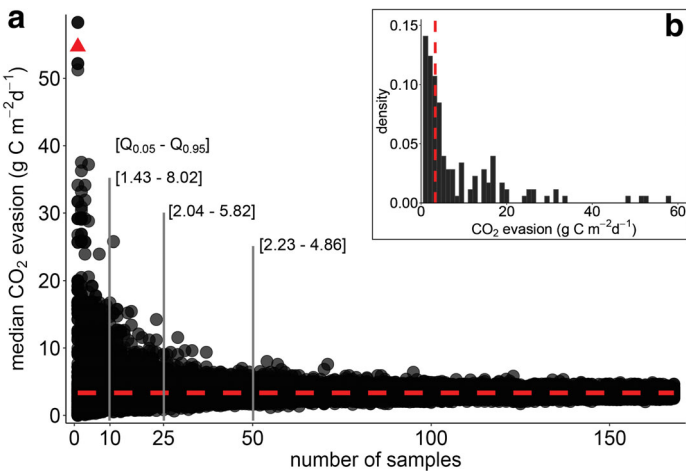


Fig. 5. (a) The median CO₂ evasion obtained by bootstrapping the population of CO₂ evasion observed, with a sampling number ranging from 1 to 168, and 200 replicates for each number of samples. The numbers in parentheses show the 5th–95th percentiles for 10, 25, and 50 samples. The red triangle shows the CO₂ evasion if calculated with the measured pCO₂ at the monitoring station close to the outlet, and median k_{600} of the catchment. The red dashed line shows the median CO₂ evasion, also in the histogram of the observed CO₂ evasion rates (b).

at spatial resolution too low to capture the variations we described (about 3000 km²). This indicates that the global estimates of riverine CO₂ evasion may be overestimated if they fail to capture spatial patterns of pCO₂ and k_{600} at the same fine spatial scales.

In summary, we find three critical shortcomings that hinder our ability to generate accurate predictions of CO₂ evasion from streams: first, the high spatial variability per se in CO₂ evasion and its parameters across stream networks. Second, the use of different scales to summarize the main variables that predict CO₂ evasion, and third, the lack of tools to predict pCO₂ across stream networks. Thus, our results suggest that the mismatch between the current global estimates of riverine CO₂ evasion (0.7–1.8 Pg C yr⁻¹; Raymond et al. 2013; Lauerwald et al. 2015), and the recent reviewed value of 3.9 Pg C yr⁻¹ (Drake et al. 2017) is partly due to the shortcomings we identified. We are aware of the unfeasibility of an extensive sampling program at the spatial scale that we identified (1 km²). Therefore, we suggest that, to advance our knowledge of the role of inland waters in the C cycle, we should move beyond accounting techniques of upscaling, and rather develop mechanistic models anchored by topographic features that govern both inputs and exchange of CO₂ (Fig. 4).

References

- Allen, G. H., and T. Pavelsky. 2018. Global extent of rivers and streams. *Science*. **361**: 585–588. doi:[10.1126/science.aat063](https://doi.org/10.1126/science.aat063)
- Battin, T. J., L. A. Kaplan, S. Findlay, C. S. Hopkinson, E. Martí, A. I. Packman, J. D. Newbold, and F. Sabater. 2008. Biophysical controls on organic carbon fluxes in fluvial networks. *Nat. Geosci.* **1**: 95–100. doi:[10.1038/ngeo101](https://doi.org/10.1038/ngeo101)
- Borges, A. V., and others. 2015. Globally significant greenhouse-gas emissions from African inland waters. *Nat. Geosci.* **8**: 637–642. doi:[10.1038/ngeo2486](https://doi.org/10.1038/ngeo2486)
- Butman, D., and P. A. Raymond. 2011. Significant efflux of carbon dioxide from streams and rivers in the United States. *Nat. Geosci.* **4**: 839–842. doi:[10.1038/ngeo1294](https://doi.org/10.1038/ngeo1294)
- Cole, J. J., and others. 2007. Plumbing the global carbon cycle: Integrating inland waters into the terrestrial carbon budget. *Ecosystems* **10**: 171–184. doi:[10.1007/s10021-006-9013-8](https://doi.org/10.1007/s10021-006-9013-8)
- Crawford, J. T., M. M. Dornblaser, E. H. Stanley, D. W. Clow, and R. G. Striegl. 2015. Source limitation of carbon gas emissions in high-elevation mountain streams and lakes. *J. Geophys. Res. Biogeosci.* **120**: 952–964. doi:[10.1002/2014JG002861](https://doi.org/10.1002/2014JG002861)
- Crawford, J. T., E. H. Stanley, M. M. Dornblaser, and R. G. Striegl. 2016. CO₂ time series patterns in contrasting headwater streams of North America. *Aquat. Sci.* **79**: 473–486. doi:[10.1007/s00027-016-0511-2](https://doi.org/10.1007/s00027-016-0511-2)
- Demars, B. O. L. 2018. Hydrological pulses and burning of dissolved organic carbon by stream respiration. *Limnol. Oceanogr.* **64**: 406–421. doi:[10.1002/limo.11048](https://doi.org/10.1002/limo.11048)
- Demars, B. O. L., J. Thompson, and J. R. Manson. 2015. Stream metabolism and the open diel oxygen method: Principles, practice, and perspectives. *Limnol. Oceanogr.: Methods* **13**: 356–374. doi:[10.1002/lom3.10030](https://doi.org/10.1002/lom3.10030)
- Drake, T. W., P. A. Raymond, and R. G. M. Spencer. 2017. Terrestrial carbon inputs to inland waters: A current synthesis of estimates and uncertainty. *Limnol. Oceanogr.: Lett.* **3**: 132–142. doi:[10.1002/lol2.10055](https://doi.org/10.1002/lol2.10055)
- Duvert, C., D. E. Butman, A. Marx, O. Ribolzi, and L. B. Hutley. 2018. CO₂ evasion along streams driven by groundwater inputs and geomorphic controls. *Nat. Geosci.* **11**: 813–818. doi:[10.1038/s41561-018-0245-y](https://doi.org/10.1038/s41561-018-0245-y)
- Hartmann, J., R. Lauerwald, and N. Moosdorff. 2014. A brief overview of the GLObal RIver Chemistry database, GLORICH. *Procedia Earth Planet. Sci.* **10**: 23–27. doi:[10.1016/j.proeps.2014.08.005](https://doi.org/10.1016/j.proeps.2014.08.005)
- Hotchkiss, E. R., R. O. Hall Jr., R. A. Sponseller, D. Butman, J. Klaminder, H. Laudon, M. Rosvall, and J. Karlsson. 2015. Sources of and processes controlling CO₂ emissions change with the size of streams and rivers. *Nat. Geosci.* **8**: 696–699. doi:[10.1038/ngeo2507](https://doi.org/10.1038/ngeo2507)
- Hotchkiss, E. R., S. Sadro, and P. C. Hanson. 2018. Toward a more integrative perspective on carbon metabolism across lentic and lotic inland waters. *Limnol. Oceanogr.: Lett.* **3**: 57–63. doi:[10.1002/lol2.10081](https://doi.org/10.1002/lol2.10081)
- Jankowski, K., D. E. Schindler, and P. J. Lisi. 2014. Temperature sensitivity of community respiration rates in streams is associated with watershed geomorphic features. *Ecology* **95**: 2707–2714. doi:[10.1890/14-0608.1](https://doi.org/10.1890/14-0608.1)
- Johnson, M. S., M. F. Billett, K. J. Dinsmore, M. Wallin, K. E. Dyson, and R. S. Jassal. 2010. Direct and continuous measurement of dissolved carbon dioxide in freshwater aquatic systems—method and applications. *Ecohydrology*. **3**: 68–78. doi:[10.1002/eco.95](https://doi.org/10.1002/eco.95)

- Keller, E. A., and W. N. Melhorn. 1978. Rhythmic spacing and origin of pools and riffles. *Geol. Soc. Am. Bull.* **89**: 723–730. doi: [10.1130/0016-7606\(1978\)89<723:RSAOOP>2.0.CO;2](https://doi.org/10.1130/0016-7606(1978)89<723:RSAOOP>2.0.CO;2)
- Kuglerová, L., A. Ågren, R. Jansson, and H. Laudon. 2014. Towards optimizing riparian buffer zones: Ecological and biogeochemical implications for forest management. *For. Ecol. Manage.* **334**: 74–84. doi: [10.1016/j.foreco.2014.08.033](https://doi.org/10.1016/j.foreco.2014.08.033)
- Lauerwald, R., G. G. Laruelle, J. Hartmann, P. Ciais, and P. A. G. Regnier. 2015. Spatial patterns in CO₂ evasion from the global river network. *Global Biogeochem. Cycles* **29**: 534–554. doi: [10.1002/2014GB004941](https://doi.org/10.1002/2014GB004941)
- Leith, F. I., K. J. Dinsmore, M. B. Wallin, M. F. Billett, K. V. Heal, H. Laudon, M. G. Öquist, and K. Bishop. 2015. Carbon dioxide transport across the hillslope-riparian-stream continuum in a boreal headwater catchment. *Biogeosciences* **12**: 1881–1902. doi: [10.5194/bg-12-1881-2015](https://doi.org/10.5194/bg-12-1881-2015)
- Lidberg, W., M. Nilsson, T. Lundmark, and A. M. Ågren. 2017. Evaluating preprocessing methods of digital elevation models for hydrological modelling. *Hydrol. Process.* **31**: 4660–4668. doi: [10.1002/hyp.11385](https://doi.org/10.1002/hyp.11385)
- Lupon, A., B. A. Denfeld, H. Laudon, J. Leach, J. Karlsson, and R. A. Sponseller. 2019. Groundwater inflows control patterns and sources of greenhouse gas emissions from streams. *Limnol. Oceanogr.: Lett.* **1**: 1–13. doi: [10.1002/lno.11134](https://doi.org/10.1002/lno.11134)
- Marx, A., J. Dusek, J. Jankovec, M. Sanda, T. Vogel, R. van Geldern, J. Hartmann, and J. A. C. Barth. 2017. A review of CO₂ and associated carbon dynamics in headwater streams: A global perspective. *Rev. Geophys.* **55**: 560–585. doi: [10.1002/2016RG000547](https://doi.org/10.1002/2016RG000547)
- Montgomery, D. R. 1999. Process domains and the river continuum. *J. Am. Water Resour. Assoc.* **35**: 397–410. doi: [10.1111/j.1752-1688](https://doi.org/10.1111/j.1752-1688)
- Natchimuthu, S., M. B. Wallin, L. Klemedtsson, and D. Bastviken. 2017. Spatio-temporal patterns of stream methane and carbon dioxide emissions in a hemiboreal catchment in Southwest Sweden. *Sci. Rep.* **7**: 39729. doi: [10.1038/srep39729](https://doi.org/10.1038/srep39729)
- Öquist, M. G., M. Wallin, J. Seibert, K. Bishop, and H. Laudon. 2009. Dissolved inorganic carbon export across the soil/stream interface and its fate in a boreal headwater stream. *Environ. Sci. Technol.* **43**: 7364–7369. doi: [10.1021/es900416h](https://doi.org/10.1021/es900416h)
- Peter, H., G. A. Singer, C. Preiler, P. Chifflard, G. Steniczka, and T. J. Battin. 2014. Scales and drivers of temporal pCO₂ dynamics in an Alpine stream. *J. Geophys. Res. Biogeosci.* **119**: 1078–1091. doi: [10.1002/2013JG002552](https://doi.org/10.1002/2013JG002552)
- Pusch, M. 1996. The metabolism of organic matter in the hyporheic zone of a mountain stream, and its spatial distribution. *Hydrobiologia* **323**: 107–118. doi: [10.1007/BF00017588](https://doi.org/10.1007/BF00017588)
- Rasilo, T., R. H. S. Hutchins, C. Ruiz-González, and P. A. del Giorgio. 2016. Transport and transformation of soil-derived CO₂, CH₄ and DOC sustain CO₂ supersaturation in small boreal streams. *Sci. Total Environ.* **579**: 902–912. doi: [10.1016/j.scitotenv.2016.10.187](https://doi.org/10.1016/j.scitotenv.2016.10.187)
- Raymond, P. A., and others. 2012. Scaling the gas transfer velocity and hydraulic geometry in streams and small rivers. *Limnol. Oceanogr.: Fluids Environ.* **2**: 41–53. doi: [10.1215/21573689-1597669](https://doi.org/10.1215/21573689-1597669)
- Raymond, P. A., and others. 2013. Global carbon dioxide emissions from inland waters. *Nature* **503**: 355–359. doi: [10.1038/nature12760](https://doi.org/10.1038/nature12760)
- Riveros-Iregui, D. A., and B. L. McGlynn. 2009. Landscape structure control on soil CO₂ efflux variability in complex terrain: Scaling from point observations to watershed scale fluxes. *J. Geophys. Res. Biogeosci.* **114**: 1–14. doi: [10.1029/2008JG000885](https://doi.org/10.1029/2008JG000885)
- Rocher-Ros, G. 2019. 1. Physico-chemical parameters measured at a high spatial resolution in the Miellajokka catchment, Sweden. 2. Paired values of CO₂ and k₆₀₀ from the GLORICH database. Swedish National Data Service Dataset [accessed 2019 February 01]. Available from <https://doi.org/10.5878/pxa2-vy55>; Available from <https://doi.org/10.5878/77ps-4f21>
- Tank, S. E., J. B. Fellman, E. Hood, and E. S. Kitzberg. 2018. Beyond respiration: Controls on lateral carbon fluxes across the terrestrial-aquatic interface. *Limnol. Oceanogr.: Lett.* **3**: 76–88. doi: [10.1002/lol2.10065](https://doi.org/10.1002/lol2.10065)
- Wallin, M., I. Buffam, M. G. Öquist, H. Laudon, and K. Bishop. 2010. Temporal and spatial variability of dissolved inorganic carbon in a boreal stream network: Concentrations and downstream fluxes. *J. Geophys. Res.* **115**: G02014. doi: [10.1029/2009JG001100](https://doi.org/10.1029/2009JG001100)
- Wallin, M., and others. 2018. Carbon dioxide and methane emissions of Swedish low-order streams—a national estimate and lessons learnt from more than a decade of observations. *Limnol. Oceanogr.: Lett.* **3**: 156–167. doi: [10.1002/lol2.10061](https://doi.org/10.1002/lol2.10061)
- Wallin, M. B., M. G. Öquist, I. Buffam, M. F. Billett, J. Nisell, and K. H. Bishop. 2011. Spatiotemporal variability of the gas transfer coefficient (K_{CO_2}) in boreal streams: Implications for large scale estimates of CO₂ evasion. *Global Biogeochem. Cycles* **25**. doi: [10.1029/2010GB003975](https://doi.org/10.1029/2010GB003975)
- Wohl, E., K. Dwire, N. Sutfin, L. Polvi, and R. Bazan. 2012. Mechanisms of carbon storage in mountainous headwater rivers. *Nat. Commun.* **3**: 1263–1268. doi: [10.1038/ncomms2274](https://doi.org/10.1038/ncomms2274)

Acknowledgments

We thank Albin Bjärhall for the help in the field survey and lab support, the Abisko Scientific Research Station for logistical support, and two anonymous reviewers for comments on an earlier version of this manuscript. We specifically thank Jens Hartmann for providing access to the GLORICH database. This study was supported by the Swedish Research Council (VR; 2013-5001) and the Swedish Research Council for Environment, Agricultural Sciences, and Spatial Planning (FORMAS; 2014-00970) to R.G.

Conflict of Interest

None declared.